Journal of Nuclear Materials 407 (2010) 48–54

Contents lists available at ScienceDirect

Journal of Nuclear Materials

journal homepage: www.elsevier.com/locate/jnucmat

Kr ion irradiation study of the depleted-uranium alloys

J. Gan [a,*], D.D. Keiser [a], B.D. Miller [b], M.A. Kirk [c], J. Rest [c], T.R. Allen [b], D.M. Wachs [a]

[a] *Idaho National Laboratory, P.O. Box 1625, Idaho Falls, ID 83415-6188, USA*
[b] *University of Wisconsin, 1500 Engineering Drive, Madison, WI 53706, USA*
[c] *Argonne National Laboratory, 9700 South Cass Ave., Argonne, IL 60439, USA*

ABSTRACT

Fuel development for the reduced enrichment research and test reactor (RERTR) program is tasked with the development of new low enrichment uranium nuclear fuels that can be employed to replace existing high enrichment uranium fuels currently used in some research reactors throughout the world. For dispersion type fuels, radiation stability of the fuel–cladding interaction product has a strong impact on fuel performance. Three depleted-uranium alloys are cast for the radiation stability studies of the fuel–cladding interaction product using Kr ion irradiation to investigate radiation damage from fission products. SEM analysis indicates the presence of the phases of interest: $U(Al, Si)_3$, $(U, Mo)(Al, Si)_3$, UMo_2Al_{20}, $U_6Mo_4Al_{43}$ and UAl_4. Irradiations of TEM disc samples were conducted with 500 keV Kr ions at 200 °C to ion doses up to 2.5×10^{19} ions/m^2 (~10 dpa) with an Kr ion flux of 10^{16} ions/m^2/s (~4.0×10^{-3} dpa/s). Microstructural evolution of the phases relevant to fuel–cladding interaction products was investigated using transmission electron microscopy.

1. Introduction

The primary objective of the RERTR program is to develop new low enrichment uranium fuels to replace the high enrichment fuels for the research and test reactors worldwide. This is a collaborative effort among many countries to ensure a safe and secured use of research and test reactors to meet non-proliferation requirement. An important part of fuel development program is to study the fuel performance under irradiation. Radiation stability of the potential fuel–cladding interaction product plays an important role in fuel performance. Microstructural characterization using transmission electron microscopy (TEM) is capable of providing important information on the microstructure (crystal structure, precipitates, defects, various interfaces and microchemistry) with resolution down to the nanometer range.

A variety of phases have the potential to develop in the irradiated RERTR fuels as a result of fuel/cladding interaction. To study the effects of radiation on the potential fuel/cladding interaction product, three depleted-uranium (DU) alloys were arc-cast with the compositions of 67U–5Si–28Al, 48U–5Mo–47Al and 69U–4Mo–20Al–7Si at the Idaho National Laboratory (INL). The first alloy composition selected is close to that of a $U(Al, Si)_3$ phase. This phase has been observed to form in uranium-silicide dispersion fuels and exhibits stable performance under irradiation [1]. The second composition is near that of $(U, Mo)Al_7$, a composition observed in interaction layers of the current version of U–Mo dispersion fuels that use aluminum as the matrix, which show poor irradiation performance at very high burn-up [2]. In order to improve the performance of U–Mo dispersion fuels, the RERTR program has been investigating the use of Si additions to the aluminum cladding matrix to influence fuel/matrix interaction such that a more stable interaction product will form. The idea is that by having Si participate in the inter-diffusion process, it is likely that a $(U, Mo)(Al, Si)_3$ phase will form and the resultant material may remain stable under irradiation, like the $U(Al, Si)_3$ phase did in the uranium-silicide fuels [3]. As a result, the third alloy has a composition near that of a $(U, Mo)(Al, Si)_3$ phase.

Many research and test reactors are operating with a water coolant at coolant temperatures less than 100 °C, such as the advanced test reactor at Idaho National Laboratory in USA. A plate type fuel normally has a thickness of approximately 1.5 mm. A thin layer of dispersion fuel about 0.5 mm thick is sandwiched with ~0.5 mm thick pure aluminum or aluminum alloy cladding on both sides. In the dispersion fuel layer, fuel particles with various diameters up to ~100 μm are embedded in the aluminum matrix. Typical peak fuel temperature is expected to be less than 200 °C. Radiation damage processes in the microstructure of RERTR fuels consist of damage due to fast neutrons and fission products. For ion irradiation studies, heavy ion irradiation with Kr ions at an ion energy of 500 keV is preferred in order to investigate microstructural response for both displacement damage and the damage associated with fission gas products [4,5].

---

* Corresponding author. Tel.: +1 208 533 7385; fax: +1 208 533 7863.
E-mail address: Jian.Gan@inl.gov (J. Gan).

0022-3115/$ - see front matter © 2010 Elsevier B.V. All rights reserved.
doi:10.1016/j.jnucmat.2010.07.008

2. Experiments

SEM images for three DU alloys after heat treatment at 500 °C for 200 h are shown in Fig. 1. The first alloy (67U–5Si–28Al) has a simple phase content with U(Al, Si)$_3$ and pure Al while the second alloy (48U–5Mo–47Al) has a more complex phase content with a mixture of UAl$_4$, UMo$_2$Al$_{20}$, U$_6$Mo$_4$Al$_{43}$ and pure Al phases. The third alloy (69U–4Mo–20Al–7Si) has a phase mixture of (U, Mo)(Al, Si)$_3$, UMo$_2$Al$_{20}$ and pure Al. The composition and crystal structure of each intermetallic phase identified in these alloys are listed in Table 1. TEM disc samples were prepared from three DU alloys through slicing, core-drilling, mechanical thinning, electrical jet-polishing and precision ion polishing. The SRIM code was used to estimate displacements per atom (dpa) for Kr ion irradiation [6]. The atomic displacement energies of 25 eV, 40 eV and 60 eV were used for Al, U and Mo, respectively. The calculated 1-dpa Kr ion fluence at a depth of 100 nm is 2.3×10^{18}, 2.4×10^{18}, 2.8×10^{18} and 2.5×10^{18} ions/m^2 for UAl$_3$ type phase, UAl$_4$, UMo$_2$Al$_{20}$ and U$_6$Mo$_4$Al$_{43}$, respectively. Since the calculated displacement damage profiles are quite similar for these phases, an average 1-dpa equivalent ion fluence of 2.5×10^{18} ions/m^2 was used for all of the five phases.

The TEM discs of DU alloys were irradiated with 500 keV Kr ions at 200 °C to doses up to approximately 10 dpa (2.5×10^{19} ions/m^2) using the intermediate voltage electron microscope (IVEM) equipped with a Tandem accelerator at Argonne National Laboratory. The ion beam has a diameter of ~1.5 mm on the specimen. The angle between ion beam and electron beam for TEM analysis is 30°. The specimen chamber vacuum is better than 5.3×10^{-5} Pa (4.0×10^{-7} torr). A double-tilt high temperature TEM specimen

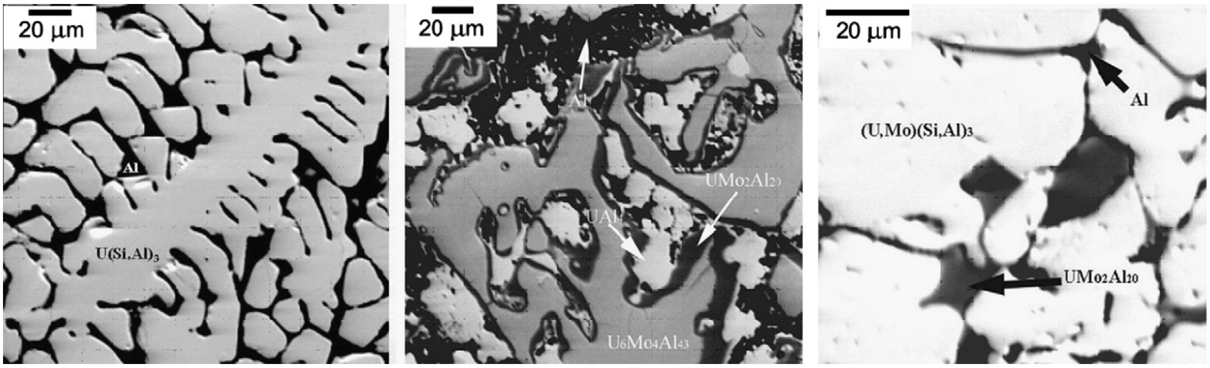

Fig. 1. SEM images of alloy 67U–5Si–28Al (left), alloy 48U–5Mo–47Al (middle) and alloy 69U–4Mo–20Al–7Si (right) show various phases of interest.

Table 1
Crystal structural information of the intermetallic phases identified in three DU alloys.

Phase	Alloy	Crystal structural information [7–10]
U(Al, Si)$_3$ U$_{27}$Si$_{13}$Al$_{60}$	67U–5Si–28Al	Cubic, L1$_2$ ordered Cu$_3$Au type, $a = b = c$ = 0.424 nm, Pearson symbol: cP4, space group: 221, T_{melt} = 1350 °C for UAl$_3$
(U, Mo)(Al, Si)$_3$ U$_{27}$Mo$_3$Si$_{19}$Al$_{49}$	69U–4Mo–20Al–7Si	Cubic, L1$_2$ ordered Cu$_3$Au type, $a = b = c$ = 0.422 nm, Pearson symbol: cP4, space group: 221
UMo$_2$Al$_{20}$ U$_5$Mo$_7$Al$_{88}$	48U–5Mo–47Al, 69U–4Mo–20Al–7Si	Cubic, $a = b = c$ = 1.4506 nm, Pearson symbol: cF184, space group: 227, T_{melt} = 1200 °C
U$_6$Mo$_4$Al$_{43}$ U$_{12}$Mo$_9$Al$_{79}$	48U–5Mo–47Al	Hexagonal, $a = b$ = 1.0966 nm, c = 1.7690 nm, c/a = 1.613, $\alpha = \beta$ = 90°, γ = 120°, Pearson symbol: hp106, space group: 193, T_{melt} = 1360 °C
UAl$_4$ U$_{22}$Al$_{78}$	48U–5Mo–47Al	Body-center orthrohomic, a = 0.6270 nm, b = 1.3710 nm, c = 0.4410 nm, $\alpha = \beta = \gamma$ = 90°, Pearson symbol: oI20, space group: 74, T_{melt} = 730 °C

Note: Both general and the measured specific composition in at.% for each phase is listed.

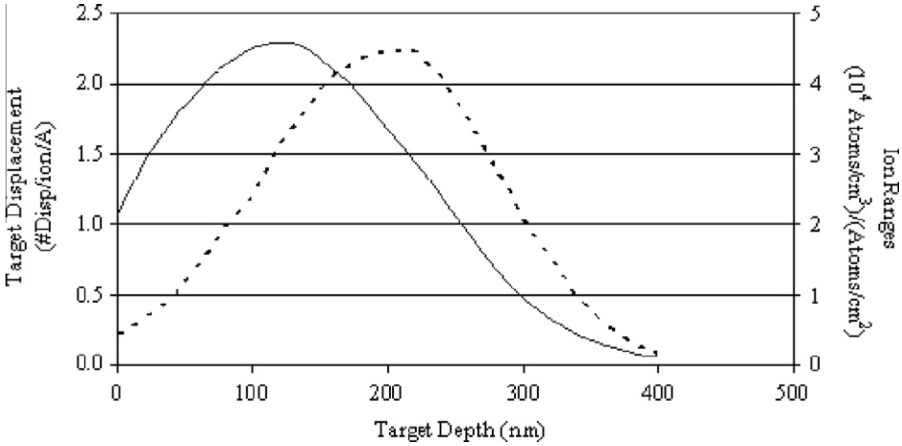

Fig. 2. Results of SRIM calculation showing target displacements (solid) and ion ranges (dash) for 500 keV Kr ions in UAl4 phase.

holder was used. Fig. 2 shows the calculated profiles of target displacements and ion ranges in UAl_4 phase. With the selected ion energy, a significant portion of the injected Kr ions was retained in the material (~15% for a 100 nm thick foil). The in situ TEM analysis was performed using a Hitachi H-9000NAR transmission electron microscope operating at 200 keV at IVEM facility. A more detailed post-irradiation microstructural characterization was conducted using a 200 keV JEOL-2010 transmission electron microscope at the Idaho National Laboratory.

3. Results

The selected area diffraction (SAD) patterns at zone direction of [0 0 1] for unirradiated (U, Mo)(Al, $Si)_3$ and U(Al, $Si)_3$ are shown in Fig. 3. While both phases have an ordered fcc crystal structure ($L1_2$ type), the latter also exhibits a super lattice structure with extra fine spots at eight times that of the lattice spacing in the U(Al, $Si)_3$ phase. Kr ion irradiation resulted in loop development in U(Al, $Si)_3$ as shown in Fig. 4. Small loops are identified at 1 dpa. At 3 dpa, some large loops with size greater than 50 nm are present. At 10 dpa, the density of loops increases and loops tangle with dislocation segments. The rel-rod dark field image did not reveal any faulted loops on {1 1 1} planes. The supper lattice structure diminished at an irradiation dose of approximately ~0.2 dpa. The U(Al, $Si)_3$ phase maintains its crystal structure with no evidence of degradation in the zone diffraction patterns with dose up to 10 dpa.

The microstructural changes as a function of irradiation dose in the phase of (U, Mo)(Al, $Si)_3$ are shown in Fig. 5. The images on the top show the SAD patterns of zone [1 2 3] while the images on the bottom show the bright field image under the same condition as in Fig. 4. At a dose of 0.25 dpa, there are small defects that have developed and a diffuse ring is visible in the SAD zone pattern. At 0.5 dpa, these defects grow in size and many spots in SAD pattern are diminished. As the irradiation proceeds to 1 dpa, the defect contrast drops to zero and the SAD pattern indicates the majority of the (U, Mo)(Al, $Si)_3$ has transformed to an amorphous state. At approximately 2 dpa, this phase becomes completely amorphous. The microstructural evolution in (U, Mo)(Al, $Si)_3$ is quite different than in U(Al, $Si)_3$ with no evidence of loop development before it turns amorphous at an irradiation dose as low as ~2 dpa. Small bubbles were found in both U(Al, $Si)_3$ and (U, Mo)(Al, $Si)_3$. No voids are found in U(Al, $Si)_3$ and (U, Mo)(Al, $Si)_3$ at doses up to 10 dpa and 4 dpa, respectively.

Bright field images showing high density of stacking faults for the unirradiated UMo_2Al_{20} phase and bubbles in UMo_2Al_{20} irradiated with Kr ions to 1 dpa and 10 dpa are shown in Fig. 6. High density stacking faults are found in the unirradiated UMo_2Al_{20} in alloy-B. The same phase in alloy 69U–4Mo–20Al–7Si shows only scattered stacking faults at much lower density. The UMo_2Al_{20} phase transforms to an amorphous phase under Kr ion irradiation at a dose of approximately 2 dpa. There is no significant change in small bubbles between 1 dpa and 10 dpa. Voids are not observed at doses up to 10 dpa. No loops were found prior to the UMo_2Al_{20} phase becoming amorphous.

For the UAl_4 phase, small defects at high density with sizes of few nanometers were found at 1 dpa as shown in Fig. 7. These small defects are believed to be responsible for the presence of

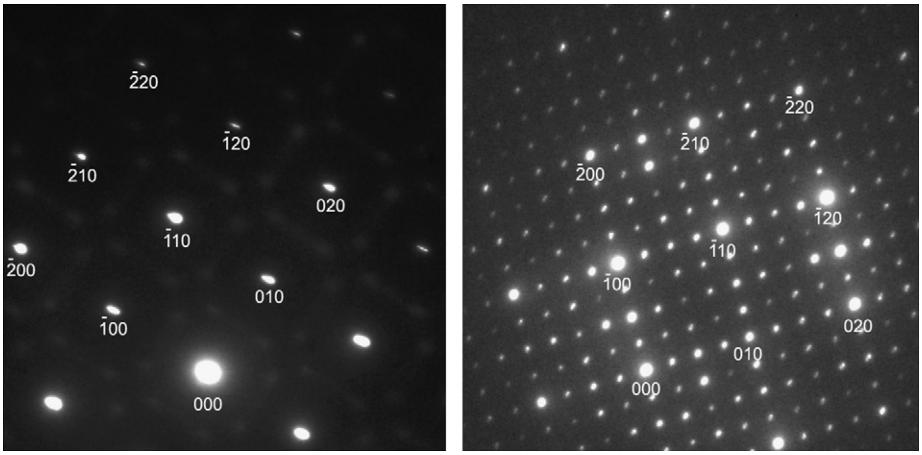

Fig. 3. The [0 0 1] zone patterns for (U, Mo)(Al, $Si)_3$ (left) and U(Al, $Si)_3$ (right). Both show the $L1_2$ ordered structure (indexed spots) with super lattice fine spots only found in U(Al, $Si)_3$.

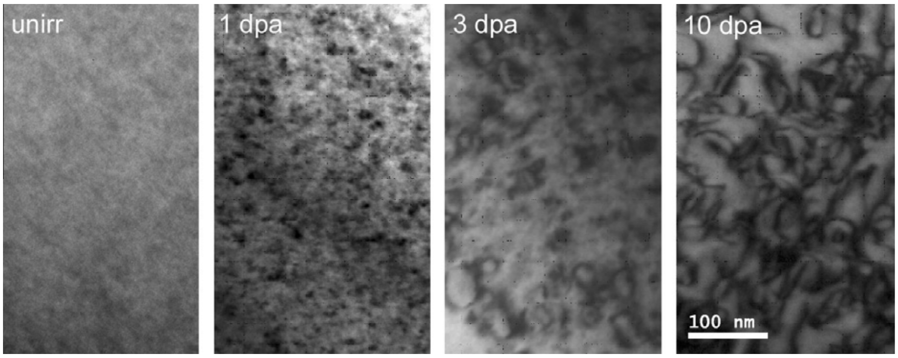

Fig. 4. Dislocation loops imaged using $g = -1, 1, -1$ in U(Al, $Si)_3$ irradiated up to 10 dpa with 500 keV Kr ions at 200 °C.

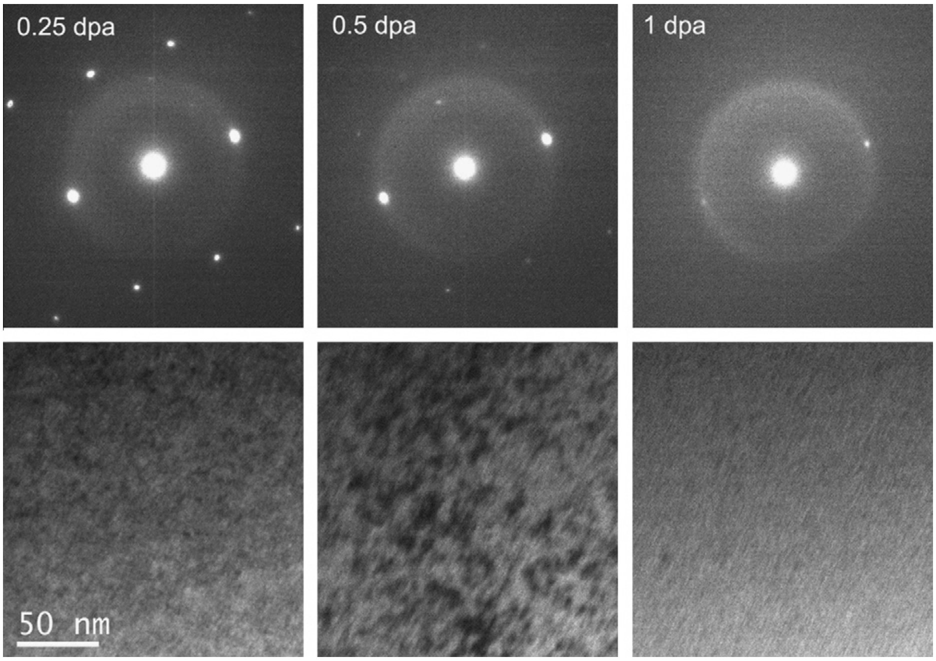

Fig. 5. SAD zone diffraction patterns ([1 2 3]) and bright field images ($g = -1, -1, 1$) in (U, Mo)(Al, Si)$_3$ as a function of irradiation dose up to 1 dpa with 500 keV Kr ions at 200 °C.

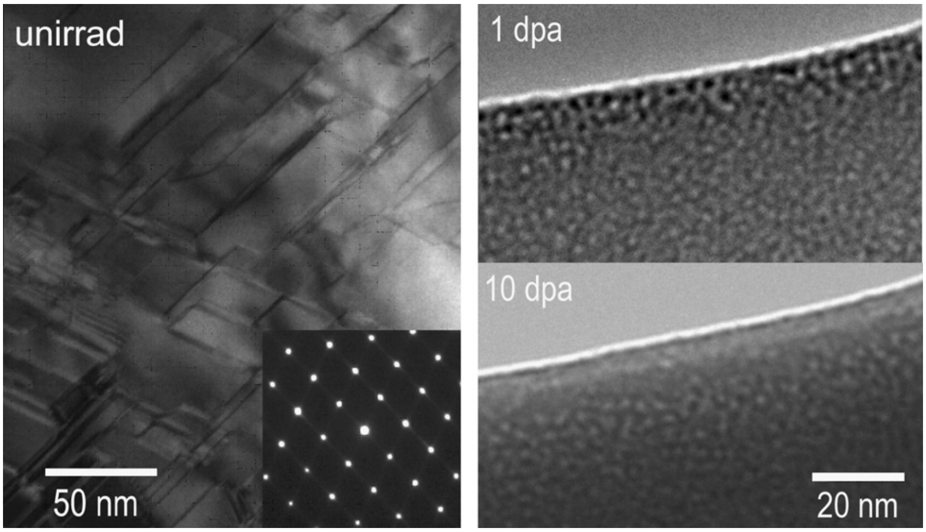

Fig. 6. Bright field image of UMo$_2$Al$_{20}$ phase near zone [0 1 1] shows the high density of stacking faults (left) and bubbles (right) at dose of 1 dpa and 10 dpa.

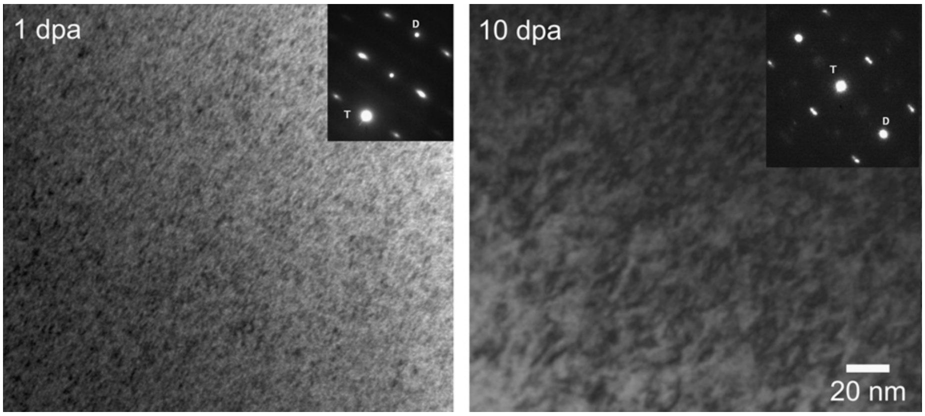

Fig. 7. Bright field images of defects in UAl$_4$ phase irradiated with 500 keV Kr at 200 °C to 1 dpa (left) and 10 dpa (right) showing high density of small defects.

streaks in the SAD patterns. The size of these small defects increases with dose up to 10 dpa. The contrast of these defects suggests that these are likely dislocation loops. Small bubbles (<2 nm) at high density are found at 1 dpa but no voids are identified at doses up to 10 dpa. The effect of Kr ion irradiation on the preexisting amorphous precipitates in UAl_4 is shown in Fig. 8. Limited composition analysis with electron-dispersive spectroscopy (EDS) reveals Mo in these precipitates. Both shrinkage and dissolution of these precipitates with irradiation dose are evident as shown in the pictures. Although UAl_4 phase retains a crystal structure at 10 dpa, the visibility of the Kikuchi line pattern drops to zero and the clarity of SAD pattern is significantly deteriorated.

For the phase of $U_6Mo_4Al_{43}$, Fig. 9 shows a bright field image and a SAD pattern at a zone direction of [3 1 1] for the unirradiated condition. The initial microstructure is clean with no sign of dislocations or precipitates. Kr ion irradiation at 200 °C quickly turns $U_6Mo_4Al_{43}$ amorphous at a dose as low as 1 dpa. Small bubbles are found at 1 dpa, but no voids are identified at 10 dpa. Due to multiple phases present in alloy 48U–5Mo–47Al, in situ TEM observation of microstructural evolution below dose of 1 dpa for $U_6Mo_4Al_{43}$ phase was not performed.

4. Discussion

Irradiations of TEM disc samples with 500 keV Kr ions at 200 °C to various doses up 10 dpa result in different microstructural response in the five phases investigated. These results may help to improve the understanding of the role of irradiated microstructure on the RERTR fuel performance, particularly on the control of fuel swelling. The discussion will follow the microstructural observation of various phases characterized before and after Kr irradiations.

The irradiation behavior of $U(Al, Si)_3$ is consistent with literature data [1]. In addition to its Cu_3Au type of ordered fcc structure ($L1_2$), the presence of a super lattice structure in the unirradiated condition has not been previously reported. Although both Al and Si atoms occupy the face center lattice sites, the appearance of superlattice spots indicates a chemical ordering rather than random occupation of the face center sites for the Al and Si atoms. This chemical ordering between Si and Al atoms in the microstructure appears not stable under irradiation. Since the super lattice diffraction spots are diminished at very low dose (around 0.2 dpa), the role of this chemical ordering on the microstructural performance

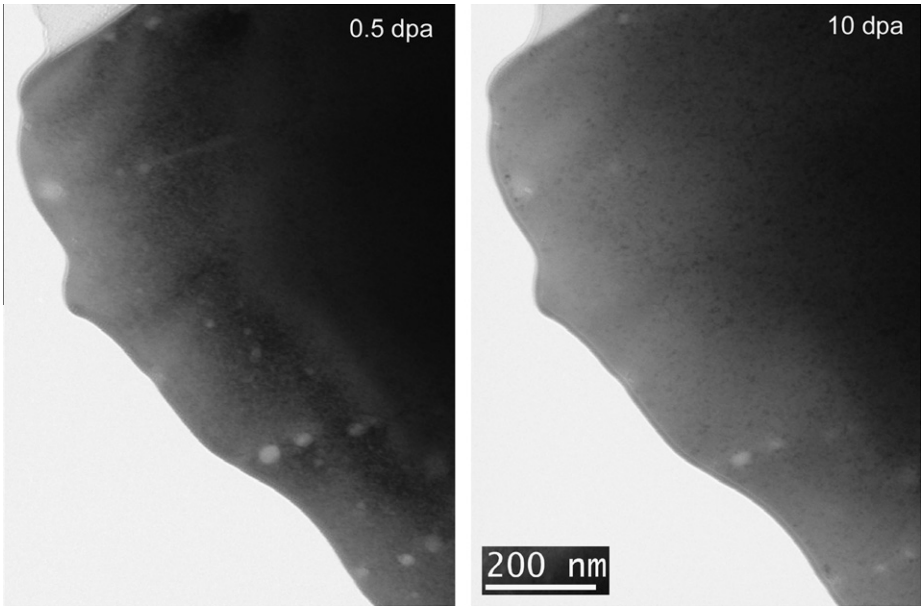

Fig. 8. Bright field images showing effect of Kr ion irradiation on precipitates in UAl_4 phase at low dose (left) and high dose (right). Shrinkage and dissolution of the precipitates are evident.

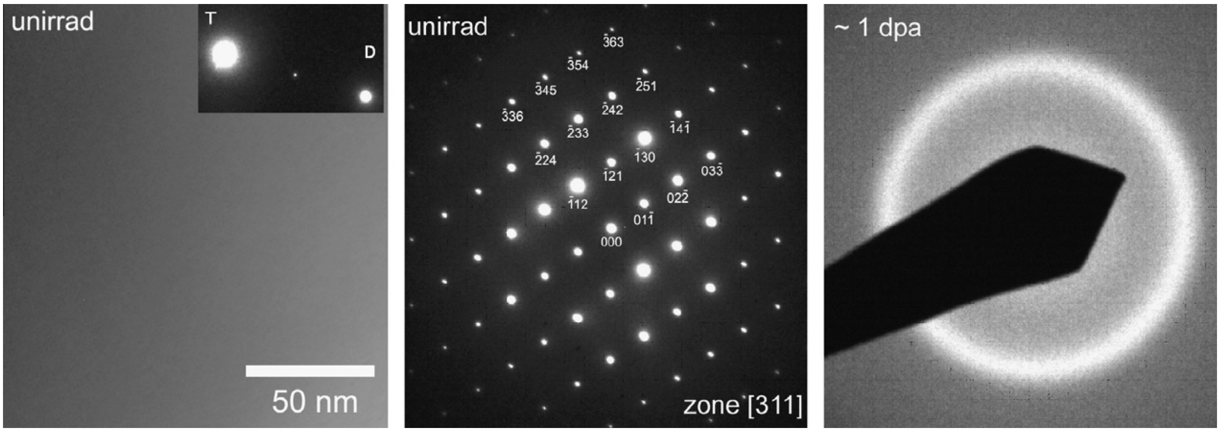

Fig. 9. Two beam bright field image (left) and SAD pattern (middle) for the unirradiated $U_6Mo_4Al_{43}$ and the SAD pattern of the irradiated (~1 dpa) (right) showing amorphization from 500 keV Kr irradiation at 200 °C.

of $U(Al, Si)_3$ under irradiation is expected to be insignificant. Considering the melting temperature of ∼1350 °C, the large loops developed at relatively low irradiation temperature at 3 dpa suggests high mobility of point defects in this phase.

It was unexpected that $(U, Mo)(Al, Si)_3$, with a similar crystal structure to $U(Al, Si)_3$, showed a very different response to Kr ion irradiation under similar conditions. Before a mature defect microstructure developed, the crystal transformed to amorphous phase at a dose of ∼1 dpa. The contrast shown in Fig. 5 at 0.5 dpa may be due to the formation of amorphous domains instead of dislocation loops. The amorphization in this phase may suggest a significantly low mobility for point defects comparing to that of $U(Al, Si)_3$ phase. Elongated spots were found in the SAD zone patterns in some of the unirradiated $(U, Mo)(Al, Si)_3$ phases, indicating crystal bending under stress. In comparison between the $U(Al, Si)_3$ and $(U, Mo)(Al, Si)_3$ phases, the measured composition in Table 1 indicates that the latter has an extra 3 at.% Mo with a stoichiometry of heavy element (U, Mo) to light element (Al, Si) as 1:2.3, rather than 1:3 for a Cu_3Au type structure. Kim reported that the addition of Mo to the interaction layer of U–Mo/Al reduces the stability of the interaction layer [11]. This result indicates that approximately 5 at.% of U or Mo atoms cannot occupy their normal lattice sites at the corners in a Cu_3Au type ordered fcc crystal structure. This may be another reasons for the structural instability in the (U, Mo) $(Al, Si)_3$ phase in this work.

Hofman proposed a correlation between fission-induced amorphization and the behavior of fission-gas driven fuel swelling. It was suggested that amorphization is responsible for an increase in fission-gas mobility and plastic flow rate of the fuel that lead to breakaway swelling [12]. If this is true, then the high dose irradiation of the $(U, Mo)(Al, Si)_3$ phase should result in relatively aggressive swelling. Keiser et al. reported the presence of $(U, Mo)(Al, Si)_3$ phase in the interaction layer of the as-fabricated dispersion fuel [13]. The recent results by Keiser et al. on the irradiated dispersion fuel with ∼50% burn-up, ∼100 °C peak temperature and $\sim 3.5 \times 10^{27}$ fission/m^3 show clear correlation between Si content and fission gas bubbles [14]. Fission gas bubbles are found in the Si depleted zone but not in the neighboring zones with relatively high Si content in the interaction layer. It may be possible that Si atoms in the $U(Al, Si)_3$ type interaction layer reduce the mobility of fission gaseous atoms. The high Si content in the interaction layer may also increase the material surface energy, thus inhibiting bubble growth. These effects may compete with the effects of amorphization and slow down the swelling driven by fission gas.

On the other hand, Rest [15] has shown that the viscosity of an irradiated amorphous material depends on the composition. Rest [16] has also related the gas-driven swelling of the amorphous material to the viscosity. A relatively high Si content may increase the viscosity of the irradiated material and, thus, limit the growth of the fission gas bubbles.

The microstructural response of UMo_2Al_{20} phase under Kr ion irradiation is consistent with the literature data. The high density stacking faults found in this phase in alloy 48U–5Mo–47Al but not in alloy 69U–4Mo–20Al–7Si demonstrates the effect of alloy fabrication on the microstructure of the individual phase. Specifically, it suggests low stacking-fault energy in the UMo_2Al_{20} phase. This crystal has a very large simple cubic cell with 184 atoms in a very complex arrangement [17]. Lack of defect feature development except for stacking faults may be related to its complex structure. This phase begins transforming to amorphous at ∼2 dpa and becomes fully amorphous at ∼10 dpa. The little change on small bubbles between 1 dpa and 10 dpa may suggest low mobility of Kr atoms in the material that may inhabit bubble coarsening. The visibility of the small bubbles at 10 dpa degrades likely as a result of amorphization.

The UAl_4 phase is the low melting point phase among the five phases investigated. The irradiation temperature of 200 °C may be too high ($T_{irr}/T_m = 0.47$) for it to undergo an amorphous transformation. Significant radiation damage in this phase is evident as the visibility of Kikuchi line patterns drops to zero and clarity of SAD patterns is degraded. UAl_4 phase may become unstable before it reaches high dose of ∼100 dpa. The heavy ion irradiation study by Wieschalla et. al. using 120 MeV Iodine ions at 200 °C in dispersion fuel (U–6Mo or U–10Mo dispersed in Al) indicated that the irradiation induced fuel/cladding interaction layer contains multiple phases of UAl_2, UAl_3 and UAl_4 [18]. They concluded that the large fraction of brittle UAl_4 phase that tends to crack under stress in the interaction layers is responsible for the breakaway swelling observed in the reactor irradiated dispersion fuel. The high dose Kr ion irradiation of UAl_4 will be helpful to verify this assumption. The presence of Mo rich amorphous precipitates in the unirradiated UAl_4 has not been previously reported. These precipitates could be a result of artifact from alloy preparation. The observed shrinkage and dissolution of these precipitates suggest that they are not stable under irradiation.

The $U_6Mo_4Al_{43}$ phase showed as the most unstable phase among five phases under Kr ion irradiation. The initial microstructure of this phase is clean and featureless. Irradiation-induced amorphization occurred at quite low dose and the phase became completely amorphous at ∼1 dpa. Since no in situ microstructural observation was made during the irradiation due to multiple phases present in the alloy 48U–5Mo–47Al, the information on microstructural development in this phase below 1 dpa is not available. Nevertheless, the early complete amorphization of this phase is consistent with its anticipated unstable microstructure in response to the irradiation.

The results from this work indicate that the microstructural stability of these five phases, ranking from the stable to the unstable, are $U(Al, Si)_3$, UAl_4, UMo_2Al_{20}, $(U, Mo)(Al, Si)_3$ and $U_6Mo_4Al_{43}$. Although small bubbles of ∼2 nm are found in some of these phases, none of these phases develop to voids at the maximum dose of 10 dpa. The large sink strength due to large surface-to-volume ratio for a thin TEM foil, low mobility of Kr atoms in the materials and the high sink strength as a result of high density small bubbles may delay or inhabit the development from bubble to voids. It is desirable to conduct high dose Kr ion irradiation ($\sim 10^2$ dpa) to link the early microstructural development to the final swelling behavior.

5. Conclusions

Three DU alloys were cast with five phases relevant to fuel/cladding interaction product in RERTR dispersion fuels. The effectiveness of the use of Kr ion irradiation to investigate the irradiation-induced damage to the microstructure from fission has been demonstrated. Among the five phases investigated, $U(Al, Si)_3$ is identified as the most stable phase up to 10 dpa with well developed dislocation microstructure. The $U_6Mo_4Al_{43}$ is the least stable phase that turns fully amorphous below 1 dpa. The UAl_4 is relatively stable and retains its crystalline structure at 10 dpa, although significant degradation due to radiation damage is evident in its zone diffraction pattern. The ternary phase of UMo_2Al_{20} is also relatively unstable as expected and becomes amorphous at a dose of approximately 2 dpa. The $(U, Mo)(Al, Si)_3$ phase is less stable than UMo_2Al_{20} and transforms to amorphous at a dose of ∼1 dpa. It is believed that the addition of Mo and the deviation from the stoichiometry for a Cu_3Au type structure are responsible for its structural instability under Kr ion irradiation. The relatively high content of Si in this phase is expected to play an important role in controlling swelling driven by fission gas.

6. US department of energy disclaimer

This information was prepared as an account of work sponsored by an agency of the US Government. Neither the US Government nor any agency thereof, nor any of their employees, makes any warranty, express or implied, or assumes any legal liability or responsibility for the accuracy, completeness, or usefulness of any information, apparatus, product, or process disclosed, or represents that its use would not infringe privately owned rights. References herein to any specific commercial product, process, or service by trade name, trademark, manufacturer, or otherwise, does not necessarily constitute or imply its endorsement, recommendation, or favoring by the US Government or any agency thereof. The views and opinions of authors expressed herein do not necessarily state or reflect those of the US Government or any agency thereof.

Acknowledgements

The authors would like to express their gratitude to Pete M. Baldo and Edward A. Ryan at Argonne National laboratory IVEM facility for the Kr ion irradiation. This work was supported through funding provided by the US Department of Energy (DOE) to the RERTR Program at the Idaho National Laboratory, operated by Battelle Energy Alliance, LLC, under DOE Idaho Operations Office Contract DE-AC07-05ID14517.

References

[1] A. Leenaers, S. Van den Berghe, E. Koonen, P. Jacquet, C. Jarousse, B. Guigon, A. Ballangny, L. Sannen, J. Nucl. Mater. 327 (2004) 121.

[2] A. Leenaers, S. Van den Berghe, E. Koonen, P. Jacquet, C. Jarousse, F. Huet, M. Trotabas, M. Boyard, S. Guillot, L. Sannen, M. Verwerft, J. Nucl. Mater. 335 (2004) 39.

[3] Y.S. Kim, G. L. Hofman, H. J. Ryu, J. Rest, Thermodynamic and metallurgical considerations to stabilizing the interaction layers of U–Mo/Al dispersion fuel, in: Proceedings of the International Meeting on RERTR, Boston, USA, November 6–10, 2005.

[4] R.C. Birtcher, R.S. Averback, T.H. Blewitt, J. Nucl. Mater. 75 (1978) 167.

[5] R.C. Birtcher, C.W. Allen, L.E. Rehn, G.L. Hofman, J. Nucl. Mater. 152 (1988) 73.

[6] J.F. Ziegler, J.P. Biersack, U. Littmark, The Stopping and Range of Ions in Solid, Pergamon Press, New York, 1996.

[7] ©2008 International Center for Diffraction Data, data card ID No. of 00-051-0930, 00-047-1106, 00-048-1355 and 00-050-1516.

[8] A.E. Dwight, A Study of the Uranium–Aluminum–Silicon System, ANL Report: ANL-82-14, September 1982.

[9] H. Noel, O. Tougait, S. Dubois, J. Nucl. Mater. 389 (2009) 93–97.

[10] D. Stahl, Fuels for Research and Test Reactors, Status Review: July 1982, ANL Report: ANL-83-5, December 1982.

[11] Y.S. kim, G.L. Hofman, H.J. Ryu, J. Rest, Thermodynamic and metallurgical considerations to stabilizing the interaction layers of U–Mo/Al dispersion fuel, in: Proceeding of the 2005 International Meeting on RERTR, Boston, USA, November 6–10, 2005.

[12] G.L. Hofman, J. Nucl. Mater. 140 (1986) 256.

[13] D.D. Keiser, Jr., J.F. Jue, J. Gan, A.B. Robinson, B.D. Miller, Characterization of Si-rich layers in as-fabricated and as-irradiated RERTR dispersion fuel plates: recent results, in: The RERTR-2008 30th International Meeting on Reduced Enrichment For Research and Test Reactors, October 5–9, 2008, Washington DC, USA.

[14] D.D. Keiser, Jr., A.B. Robinson, J.F. Jue, P. Medvedev, M.R. Finlay, Characterization of the microstructure of irradiated U–Mo dispersion fuel with a matrix that contains Si, in: The 13th Annual Topical Meeting on Research Reactor Fuel Management (RRFM) 2009 in Vienna, Austria, March 22–25, 2009.

[15] J. Rest, Comput. Mater. Sci. 44 (2008) 207–217.

[16] J. Rest, J. Nucl. Mater. 325 (2004) 107–117.

[17] S. Niemann, W. Jeitschko, J. Solid State Chem. 114 (1995) 337.

[18] N. Wieschalla, W. Petry, A. Rohrmoser, P. Boni, K. Boning, A. Bergmaier, G. Dollinger, R. Grobmann, J. Schneider, Heavy ion irradiation of U–Mo/Al dispersion fuel, September 9, 2005.